International Journal of Innovative Technology and Exploring Engineering (IJITEE)
ISSN: 2278-3075 (Online), Volume-9 Issue-3, January 2020

Tumor Segmentation using Optimize Evidential C-Means at Brain MRI Images

Nagaveni B Sangolgi, M. Sasikala

Abstract: ***The accurate treatment of tumor is the major key for diagnosis and therapy, so the development in an area of image processing provide greater contribution in order to detect the tumors in human brain. A medical imaging technique such as MRI is generally used to capture the human brain images. In this paper, we addressed a PbET that is very effective process for reasoning and modelling with the presence of imprecise information and uncertainty. In the PbET function, we will propose an Optimize Evidential C-Means (OECM) approach for the delineation of Gliomas tumor in a MRI brain images. An OECM approach is integrated with spatial regularization and LM for the tumor segmentation in MRI brain image, where the LM is consider to measure the distance for better representation of comparisons between surrounding voxels and the clustering distortion. In order to validate our proposed model, we compared with different brain tumor segmented approach in terms of dice coefficient and sensitivity.***

Keywords: Magnetic Resonance Imaging (MRI), Probability based Evidence Theory (PbET), Learning Metric (LM), Optimize Evidential C-Means (OECM)

I. INTRODUCTION

Whenever the damaged or old cells die, the new cells replace that cells old cells and sometimes it don't die, but the new cell got generated even when the human body doesn't require them. Therefore, body build up with extra cells (i.e., a bulk of tissue) and called as tumor. The invention and transformation in a section of image processing provide greater contribution in order to detect the tumors in human body and human brain, there are several optimize algorithms and techniques have been provided to diagnose the abnormalities present in a brain, which should be detect as early as possible with the appropriate information of disease. MRI (Magnetic Resonance Imaging) is a medical imaging technique, generally used to capture the human brain images and this one preferred over the CT (i.e., Computed Tomography) due to its more detailed informative image of brain tumor.In this study, we will use MRI image as the input that consist of Gliomas brain tumors, because the Gliomas having the higher occurrence and morality rate [1], these can be graded into two types Low-grade Gliomas (LG) and High-grade Gliomas (HG), where the HG is more infiltrative and aggressive than the LG. According to [2], the patients under treatment don't survive more than 14 months on an average rate, whereas the current treatment of tumors include radiotherapy, surgery, chemotherapy 'or' combination of them.

Revised Manuscript Received on January 30, 2020.
***** Correspondence Author
Nagaveni B Sangolgi*, Asst Prof, ECE Dept, Faculty of Engg and Technolgy (Ex- women), Sharnbasva University, Kalaburagi.
Dr. M. Sasikala, Principal, Godutai Enginerring College For women, kalaburagi.

In clinical practice, the MRI is very useful to evaluate Gliomas and meanwhile it is probable to obtain MRI sequences by complementary information. The precise Gliomas segmentation and the structures of intra tumoral is very necessary for the treatment planning, but also for the follow up evaluations, whereas the manualsegmentation consumes lots of time and causes to intra and inter rate errors which is difficult to characterize. Therefore, the physicians uses rough measurement for assessment, due to this case, we require accurate semi-auto measurement or full automatic measurement technique [1] [3]. However, the difficulty arises due to the higher variability of shape, location and structure; also, the arrangement of tumor mass changes the surrounding of normal tissues [3] In addition, the MRI image consist of some difficulty like as inhomogeneity intensity [4] 'or' different range of intensity among the acquisition scanners [5]. In segmentation process of brain tumor, there are several technique that explicitly progress a parametric 'or' non parametric probability model for fundamental data, also these techniques generally exhibits likelihood function that corresponds to prior and observational model. Considering these abnormalities, the tumors can be segmented such as the normal tissue outliers and subjected to connectivity and shape constraints [6]. A variety of techniques depends upon probabilistic atlases [7] [8], in this type of brain tumors, the estimation of atlas in necessary at segmented time due to its dynamic location and shape of neoplasms. The effect of mass can be used to estimate the growth of tumor, also useful to optimize the atlases [8], the surrounding of voxels is useful to provide information to achieve better-segmented result by MRF (Markov Random Fields) [7]. In paper [3], provided a MRF technique for brain tumor segmentation using the MRI images, initially the super voxels pre-processing step is performed which estimate based upon a histogram method with likelihood function. However, a generative model is used to generalize better in unsupervised data [3], but it causes difficulty in order to provide explicitly prior information into a suitable probabilistic model.Another type of approaches learns directly from the distribution of data, although a training step can provide disadvantage and these approach can acquire patterns of brain tumor which don't follow some specific model. Therefore, these type of methods generally consider voxels as the identically and independent distribution [9], but the information of context can be provided via the features, which causes some small clusters 'or' isolated voxels can be incorrectly classified with wrong class labels (i.e., sometimes in anatomically and physiological unlikely locations). While considering the textural features [10] [11], the spatial location surrounds each of the voxel are very possible to offer complementary information in order to more appropriate segmentation.

However, including of textures causes difficulty in tumor segmentation due to that huge amount of textures extraction, in addition, several extracted features are may be undependable or imprecision due to the blurred and noisy medical images. The researchers in [12] [13], shown that the adaptation of distance metric to handle data effectively in order to improve the clustering algorithm performance. However, but there are not such existing methods which provide efficient segmentation of high dimensional data that consist of unreliable input feature and causes the performance degradation with this type of inappropriate information.In this study, we are addressing a PbET, which is very effective process for reasoning and modelling with the presence of imprecise information and uncertainty, also has been concluded to have larger expressive power [14]. In the PbET function, we will propose a novel clustering approach for the delineation of Gliomas tumor in a MRI brain images. The major contribution of our proposed model can be given as; initially texture features are added as the complementary information in a proposed model to get more appropriate segmentation. Moreover, the Learning Metric (LM) is consider to measure the distance for better representation of comparisons between surrounding voxels and the clustering distortion instead of using Euclidean distance respectively. In addition, a sparsity based constraint is considered in LM updating process to provide a feature selection procedure through a low dimensional transformation of feature, which limit the properties of unnecessary input features on segmented outcome. Afterwards, a novel energy function is integrated in PbET using the MRF, because it provide reliable method to obtain spatial information [15], this novel MRF dependent energy function is included in OECM and effectively provide the spatial regularization at MRI brain images.

II. RELATED WORK

Accurate and early treatment of tumor is the major key for diagnosis and therapy, whereas earlier computer based treatment depends upon handcrafted feature from MRI that are generally difficult and inaccurate. There are several Glioma segmentation approaches have been generated and proposed based upon the some type of pathology properties, in general these categories are sub divided into two type such as; probability based approaches and non-probability based approaches. While considering the probability based approaches, the corresponding process directly learn via the association between original image feature and the segmented labels (i.e., without any kind of prior domain information) such as decision trees [16] 'or' support vector machines [17]. A deep neural-networks has adopted lots of popularity and can be applied for both classification and segmentation of tumor, where the mostly of the work considered 3D MRI like a 2D series images and uses a modality fusion methodology by performing feature concatenation. In paper [18], proposed a 3D convolutional neural network with the presence of gated multimodal unit (GMU) and afterwards the information acquired with these method used in multiple modalities. Moreover, the 3D convolutional kernels are applied to complete MRI images in order to gather sagittal abnormalities, coronal and axial directions, in addition GMU with hidden nodes is considered to add the information of several MRI modalities in decision and feature level. However, this approach majorly depends upon intensity features, with limiting the segmentation under a similar imaging protocol that used at the training data. Training the data is a time consuming process, but also uses at discriminative model in order to get the relationship. A method like generative model is also a probability type methods, which generally depends upon intensities and pixel labels; afterwards specifying the probability approach, these type of methods calculate the prior probabilistic function and likelihood class condition of the labels, which tends to simulate the considered variables (i.e., MRF) [19]. Though, the generative methodologies require full prior information in order to compute the probability function, that to indicate their problems in segmenting Gliomas. While considering non-probability based approach can be used in quicker segmentation process and require fewer information from dataset, (e.g. Fuzzy logic approach) that can be used for automatic segmentation of Glioma, but generally it only take similar type of intensity with the absence of some constraints [20]. Moreover, several type of sowed region approach is growing and excepted in field of medical image segmentation [21]. Some different type of approaches such as level set prototype [22] [23] and snake method [24] have been used in medical image segmentation, however counter model and sowed region approaches requires to adjust the counters 'or' seed points, whenever the initialization are not appropriate it causes the worst segmentation. The manual interventions and poor constraint circumstances restrict their accomplishment on large number of medical dataset, therefore a more optimize approach is require for better tumor segmentation.

III. PROPOSED METHODOLOGY

In this paper, we proposed an OECM approach that integrated with spatial regularization and LM for the tumor segmentation in MRI brain image. The collection of feature vector is consider as $\{A_1, \ldots, A_n\}$ in K^p that describe the n voxels under an area of interest (AOI), where the AOI is user defined section which includes tumor. Here we also consider that the voxels belong from hypothesis B_1 (i.e., background) or from hypothesis B_2 (i.e., positive tissue) without presence of any outliers. Therefore, the clusters of whole frame can be given as set C

$$\mathrm{C} = \{B_1, B_2\} \qquad (1)$$

Where, individual d mass function satisfies $d(B_1) + d(B_2) + d(\mathrm{C}) = 1$, without any presence of $d(\mathrm{g})$. The ambiguity is measures by $d(\mathrm{C})$ for the cluster B_1 and B_2, also the heterogeneous section and blurring boundary are assigned to $d(\mathrm{C})$.

1.1 Spatial Regularization

Considering the prior spatial information of image volume, F represent the creedal partition matrix such as $\mathrm{F} = \{d_i\}_{i=1}^{n}$, where every d_i mass function presented as random vector in K^3. Here we consider $\mathrm{G} = \{\mathrm{G}(i)\}_{i=1}^{n}$ as high dimensional neighborhood system, $\mathrm{G}(i) = \{1, \ldots, H\}$ represents the set of neighbors H of a i voxels

and the corresponding voxels masses in $\mathrm{G}(i)$ can be given as $\{d_1^i, \ldots, d_H^i\}$. While the feature vectors of considered voxels can be given as $\{A_1^i, \ldots, A_H^i\}$.

The d_i distribution is expected to dependent on presumed image dimension neighborhood system such as;

$$p\left(d_i|\{d_j\}_{j\neq i}^n\right) = p\left(d_i|\{d_h^i\}_{h\in \mathrm{G}(i)}\right) \quad (2)$$

Therefore, the distribution process of F can be given as;

$$p(\mathrm{F}) = N^{-1}\,\mathrm{e}\{-L(\mathrm{F})\} \quad (3)$$

Where, the normalizing constant can be given by Z and the energy function is given in the form of;

$$L(\mathrm{F}) = \beta \sum_{i=1}^{n} \sum_{h\in \mathrm{G}(i)} M(i,h) \quad (4)$$

Where, $\beta > 0$ is a scalar and a hyper-parameter value that controls the local homogeneity degree in a AOI, $\sum_{h\in \mathrm{G}(i)} M(i,h)$ shows for the potential function that measure the smoothness nearby voxel i. Moreover, $M(i,h)$ shows for the inconsistency between the voxel i and its neighborhood h, in PbET framework, $M(i,h)$ can be given as;

$$M(i,h) = \delta_{ih} R d_{ih}^2 \quad (5)$$

Where, Rd_{ih}^2 shows for the difference between d_H^i and d_i, while weighting factor is denoted by δ_{ih} and can be computed in a feature space. Therefore, the value of Rd_{ih}^2 in between d_H^i and d_i can be written as;

$$Rd_{ih}^2 = \left(d_i - d_H^i\right)\mathbf{J}\left(d_i - d_H^i\right)' \quad (6)$$

Where, $h \in \mathrm{G}(i)$ and $\mathbf{J}$ is a positive matrix whose values represented in the form of Jaccard indexes such as;

$$\mathbf{J}(X,Y) = |X \cap Y|/|X \cup Y|, \forall X, Y \in 2^{\mathrm{C}}\backslash \mathrm{g} \quad (7)$$

Also the $\mathbf{J}$ value can be represented as;

$$\mathbf{J} = \begin{pmatrix} 1 & 0 & 1/2 \\ 0 & 1 & 1/2 \\ 1/2 & 1/2 & 1 \end{pmatrix} \quad (8)$$

Therefore, the novel objective function of the OECM include the spatial based regularization function such as;

$$\Upsilon_{oecm}^{s}(\mathrm{F},\eta) = \sum_{i=1}^{n}\sum_{X_j=\mathrm{g}} m_j^2 d_{ij}^2 R_{ij}^2 + \beta \sum_{i=1}^{n}\sum_{h\in \mathrm{G}(i)} \delta_{ih} R d_{ih}^2 \quad (9)$$

That subjected towards constraints $d_{ij} \geq 0$ and $d_{ij} = 1$ when $\forall j \in 1, \ldots, n$. The second term in equation (9) shows for the spatial regularization, where η is prototype component and Rd_{ih}^2 computes the dissimilarity between d_H^i and d_i as per equation (6).

1.2 Learning Metric (LM)

In this subsection, we will attempt to add textural feature in OECM as the complementary info for appropriate tumor segmentation, therefore the feature selection and learning metric are the necessary process. The matrix **P** can be represented during the clustering is $\mathbf{P} \in \mathrm{K}^{p\times q}$ with constraint $q \ll p$ through dissimilarity in between two A_1 and A_2 feature vectors, and can be written as;

$$R^2(A_1, A_2) = (A_1 - A_2)\mathbf{P}\mathbf{P}'(A_1 - A_2)' \quad (10)$$

The **P** matrix transforms the initial feature space vector to low-dimensional feature subspace, where as to get the **P** matrix transforms the R_{ij}^2 distance used in (9) and can be computed using (10). While considering the voxel i and its neighborhood h, here we define the weighting factor;

$$\delta_{ih} = \left(A_i - A_h^i\right)\mathbf{P}\mathbf{P}'\left(A_i - A_h^i\right)' \quad (11)$$

Hence, based upon the analysis of (9) objective function, the updated learning metric can be given as;

$$\begin{aligned}\Upsilon_{oecm}^{mls}(\mathrm{F},\eta,\mathrm{P}) = &\sum_{i=1}^{n}\sum_{X_j=\mathrm{g}} m_j^2 d_{ij}^2 (A_i - \bar{V}_j)\mathbf{P}\mathbf{P}'(A_i - \bar{V}_j)' \\ &+ \beta \sum_{i=1}^{n}\sum_{h\in \mathrm{G}(i)} R d_{ih}^2 (A_i - A_h^i)\mathbf{P}\mathbf{P}'(A_i - A_h^i)' \\ &+ \alpha \|\mathrm{P}\|_{2,1} \\ &- \log\left((\bar{A}_{B1} - \bar{A}_{B2})\mathbf{P}\mathbf{P}'(\bar{A}_{B1} - \bar{A}_{B2})'\right)\end{aligned} \quad (12)$$

This above (12) subjected to constraint $d_{ij} \geq 0$.

$$\|\mathrm{P}\|_{2,1} = \sum_{i=1}^{p} \sqrt{\sum_{j=1}^{q} P_{i,j}^2} \quad (13)$$

The α is scalar hyper-parameter which maintain the regularization influence, in addition the last part of (12) is used to control being trivially solved at P = 0, that can cause failures of all feature vectors in a single point. Here two predetermined prototypes $\bar{A}_{B1}$ and $\bar{A}_{B2}$ vectors are consider for background and positive tissue respectively.

1.3 Optimize Evidential C-Means (OECM) Approach

The OECM approach is elaborated in this section and table 1 provide the OECM algorithm, where to control the updating metric step, we initially initialize the clusters center and mass function by original ECM approach in step 1. Afterwards a small number of voxels are automatically chosen as the seeds with cluster labels that are predefined, also based on the previous mass function the classification of image voxels are done into three clusters such as $\{B_1\}$, $\{B_2\}$ and $\{\mathrm{C}\}$. In addition, to ensure the selected number of seeds and reliability, the seeds of tumor are determined like a voxel,

where intensity of values are greater than a third quartile voxel in B_1 cluster; whereas the background seeds are used to determined AOI boundary. Afterwards, the background seeds and mass function of tumor can be given as $d(\{B_2\}) \equiv 1$ and $d(\{B_1\}) \equiv 1$, respectively. The output dimension is represented by **P** in a q number of columns, afterwards the principle component analysis is applied to $\{A_1, \ldots, A_n\}$ feature vectors.

Table 1: OECM Algorithm

Step 1	**Input** $\{A_1, \ldots, A_n\} \in \mathrm{K}^p$ feature vectors is considered, $\mathrm{G}(i)$ is spatial neighborhood of i voxel; β and α are the hyper parameters; $\mathrm{F}^{(0)}, \eta^{(0)}$ and $\mathrm{P}^{(0)}$ are initialize to initial phase.
	for $l = 1, 2, \ldots$ **do**
Step 2	The efficient interior approach is used to calculate $\mathrm{F}^{(l)}$ with equation (14), $\mathrm{F}^{(l-1)}, \eta^{(l-1)}$ and $\mathrm{P}^{(l-1)}$
Step 3	$\eta^{(l)}$ calculate according to equation (18) and $\mathrm{F}^{(l)}$
Step 4	$\mathrm{P}^{(l)}$ calculate according to proximal gradient approach with (19); $\mathrm{F}^{(l)}, \eta^{(l)}$ and $\mathrm{P}^{(l-1)}$;
Step 5	**if** no change in Υ_{oecm}^{mls} **then**; break;
	End
	End
Step 6	The final vectors $\mathrm{F}^{(*)}, \eta^{*}$ and $\mathrm{P}^{(*)}$

While in step-2, the minimization of (12) relates towards first two values that turns to be quadratic difficulty with respect to function of mass $\mathrm{F} = (d_{ij})$, and the derivative also concentrating on mass function $d_i \in \mathrm{K}^3, \forall i \in 1, \ldots, n$, can be given as;

$$\frac{\partial \Upsilon_{oecm}^{mls}}{\partial d_i} = 2d_i\vartheta + 2\beta \sum_{j \in \mathrm{G}(i)} R_{ij}^2 (d_i - d_j)\mathbf{J} \quad (14)$$

Where, the **J** matrix is shown in (8), R_{ij}^2 is evaluated by (11) and ϑ is given as;

$$\vartheta = \begin{pmatrix} m_1^2 R^2(A_i, \bar{\eta}_1) & 0 & 0 \\ 0 & m_2^2 R^2(A_i, \bar{\eta}_2) & 0 \\ 0 & 0 & m_3^2 R^2(A_i, \bar{\eta}_3) \end{pmatrix} \quad (15)$$

Where, the $R^2(A_i, \bar{\eta}_1)$ is measured from (11) and; based upon the (14), efficient interior approach [25] is used to calculate $\mathrm{M}^{(l)}$ that can solve quadratic difficulty.

Considering step 3, the first term of (12) is only responsible for updating prototypes; let consider ω_j and ρ_j value as;

$$\omega_j = \sum_{i=1}^{n} m_j^2 d_{ij}^2 \quad (16)$$

$$\rho_j = \sum_{i=1}^{n} m_j^2 d_{ij}^2 A_i, \forall j \in \{1, 2, 3\} \quad (17)$$

Afterwards, the clusters centers $\{B_1\}$ and $\{B_2\}$ are computed respectively and directly as;

$$\eta_1 = 2\omega_2(2\rho_1 + \rho_3) + \omega_3(\rho_1 - \rho_2) \Big/ 4\omega_1\omega_2 + \omega_3(\omega_1 \cdot$$

$$\eta_2 = 2\omega_1(2\rho_2 + \rho_3) + \omega_3(\rho_2 - \rho_1) \Big/ 4\omega_1\omega_2 + \omega_3(\omega_1 \cdot \quad (18)$$

In step 4, excluding the third term in (12) objective function is a differentiable to perform transformation of matrix P, though the sparsity regularization (i.e., third term) is only for partially smooth at P=0 singularity. Therefore, the proximal gradient approach [26] is consider to be the effective alternative in order to resolve the metric updating difficulty and, the derivative of (12) with tends to P can be given as;

$$\frac{\partial(\cdot)}{\partial \mathrm{P}} = 2\sum_{i=1}^{n} \sum_{X_j = \emptyset} m_j^2 d_{ij}^2 (A_i - \bar{\eta}_j)\mathbf{P}(A_i - \bar{\eta}_j)' + 2\beta \sum_{i=1}^{n} \sum_{h \in \mathrm{G}(i)} R d_{ih}^2 (A_i - A_h^i)\mathbf{P}(A_i - A_h^i)' - \frac{2(\bar{A}_{B1} - \bar{A}_{B2})\mathbf{P}(\bar{A}_{B1} - \bar{A}_{B2})'}{(\bar{A}_{B1} - \bar{A}_{B2})\mathbf{P}\mathbf{P}'(\bar{A}_{B1} - \bar{A}_{B2})'} \quad (19)$$

The above equation (19) tends to provide better convergence rate and simple computational, which help to get required LM at current step.

Furthermore, the mass function and segmented performance from algorithm 1 can be extend, where the mass function $\{d_1^i, \ldots, d_H^i\}$, at each voxel i in the neighborhood $\mathrm{G}(i)$ are shows as the H independent parts of evidence at cluster label i. Here, we consider reliability of each evidence d_h^i which is inversely dependent to spatial difference between h and i, let consider the s_{ih}^2 to be spatial distance. Then based upon the evidence theory, each of the evidence piece $d_h^i, \forall h \in 1, \ldots, H$, can be weighted through a coefficient V_h;

$$V_h = \mathrm{e}(-s_{ih}^2) \quad (20)$$

So the discounted function of mass can be given as;

$$Bd_h^i(\{B_j\}) = V_h d_h^i(\{B_j\}), \forall j \in \{1, 2, \}$$
$$Bd_h^i(\{\mathrm{C}\}) = 1 - \sum_{j=1}^{2} Bd_h^i(\{B_j\}) \quad (21)$$

The discounted function of mass via (21) can be fused with a renewed mass function d_i. However, in final segmentation, only the component with higher voxels number will be considered as targeted tumor, which causes the effective handling of difficult segmentation task and tends to get a better tumor segmentation.

IV. RESULTS AND ANALYSIS

The detection and segmentation approach is implemented at MATLAB 2016b,

with the system configuration of 8 GB RAM, Intel i5 Processor and Windows 10 Operating system. The used dataset in this study is taken through Brain Tumor Segmentation (BraTS), which is available on MICCAI-2013 grand segmentation challenge [27]. This BraTS image dataset comes with several type of MRI modalities such as; T1-weighted, T1-contrast, T2-weighted, and Fluid-attenuated inversion recovery (i.e., FLAIR). In addition, it provides the ground-truth data for brain tumor that can be used to measure sensitivity and etc. In this study, we mainly focused on high grade tumor and using only MRI image modality of T1-contrast.In order to calculate the dice coefficient we using the formula as;

$$DS = (2 \times |X \cap Y|) / (|X| + |Y|) \quad (2)$$

Where, DS represent for dice score, X represent the extracted region of tumor and Y represent the ground truth.

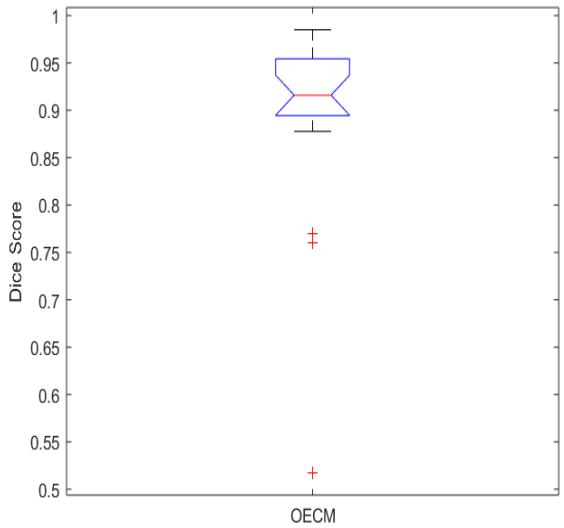

Figure IV.1 Box Plot for the Dice Coefficient

Figure 4.1 shows the Box Plot for the Dice Coefficient; the mean value of dice coefficient is obtained as 0.8939, which shows our approach provide effective segmentation for brain tumor segmentation in MRI images. The minimal and maximal value of dice coefficient were obtained as 0.517 and 0.985 respectively.

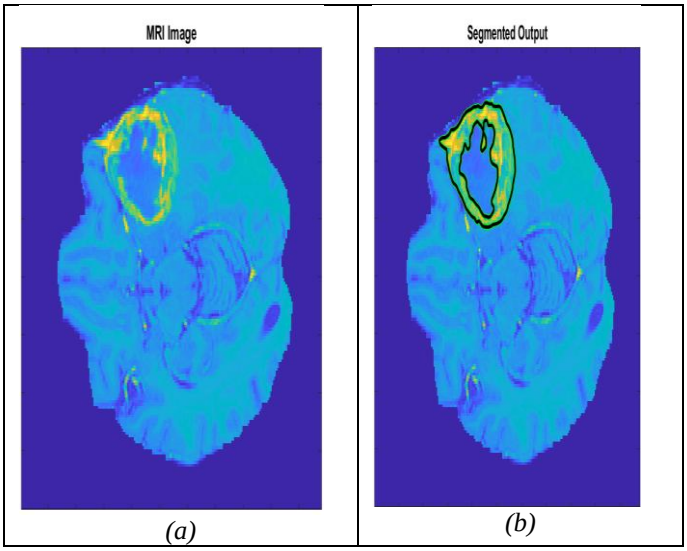

(a) *(b)*

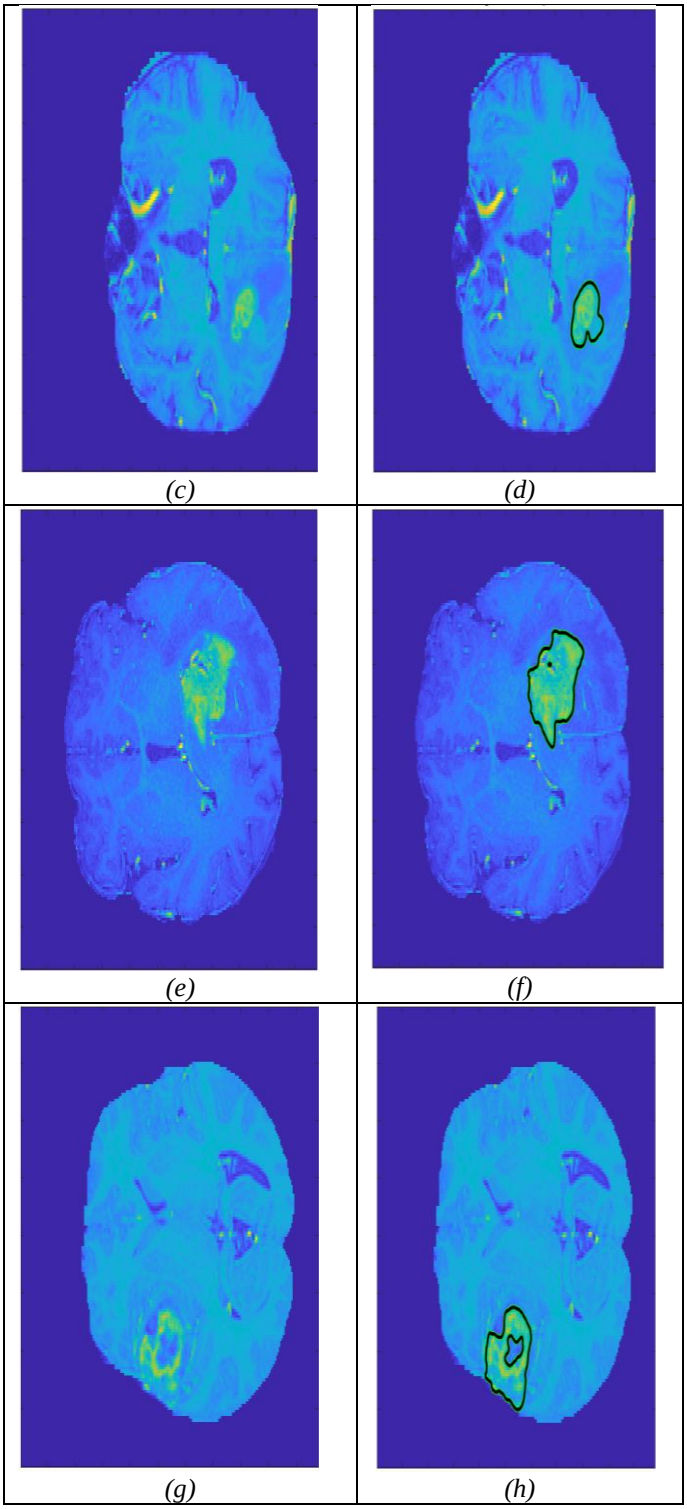

(c) *(d)* *(e)* *(f)* *(g)* *(h)*

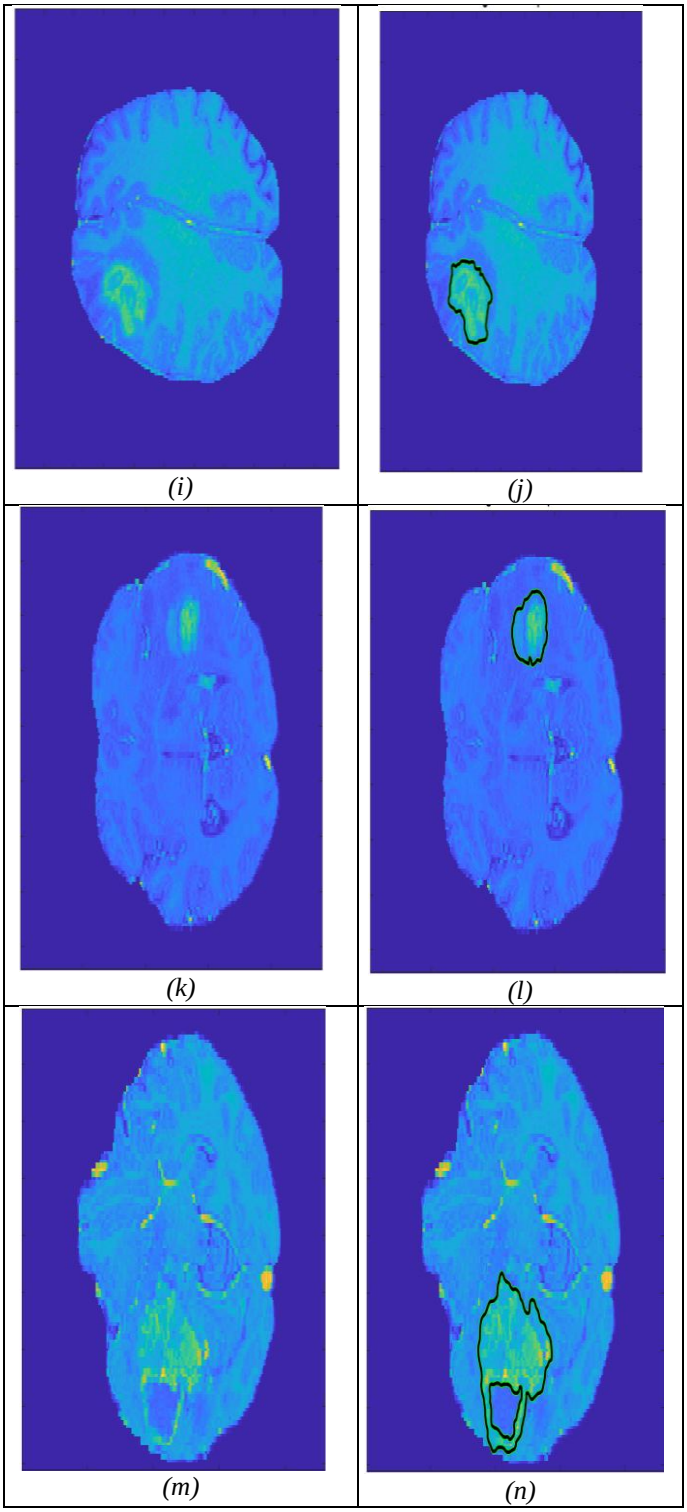

Figure IV.2: (a), (c), (e), (g), (i), (k) and (m) are the randomly selected HG-MRI Images; and their segmented outcome is represented by (b), (d), (f), (h), (j), (l) and (n), respectively.

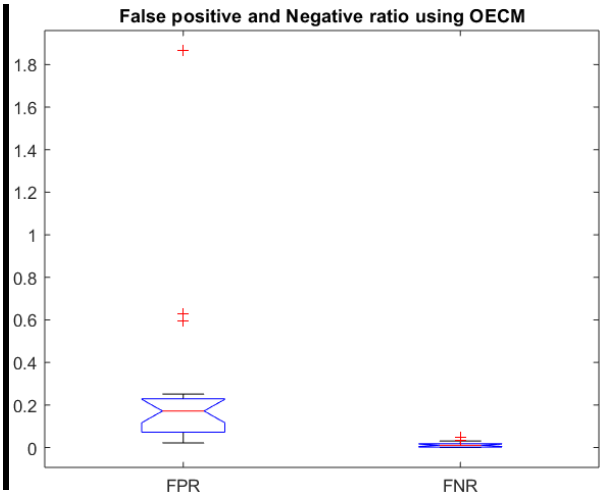

Figure IV.3: False Positive Rate (FPR) and False Negative Rate (FNR)

Figure 4.2 shows the randomly selected MRI images and their segmented outcome using our proposed OECM approach, where the first column shows the MRI images and column two represent the segmented outcome, also the black line is used to mark the tumor region in high-grade tumor. Figure 4.3 shows for the False Positive Rate (FPR) and False Negative Rate (FNR), where the average values of FPR and FNR are 0.268 and 0.012.

Table2: Mean Dice coefficient obtained through some segmentation approach

Segmentation approach	Dice Coefficient Value
LIPC [28]	0.86
CNNs [29]	0.88
Cordier et al. [30]	0.86
CTSS [31]	0.88
OECM	0.89

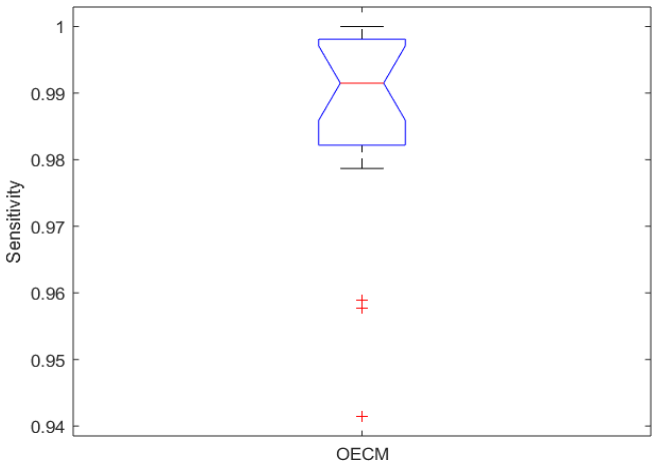

Figure IV.4: Box-Plot for Sensitivity

Table 2 shows the mean value of Dice coefficient that obtained through some segmentation approach on the BraTS datasets, where our OECM approach got 0.89 dice score which 1.12% more compare to CTSS [31] approach. Figure 4.4 shows the Box Plot for the Sensitivity; the mean value of sensitivity is obtained as 0.987, which shows the effectiveness segmentation for brain tumor by our proposed approach in MRI images. The minimal and maximal value of sensitivity were obtained as 0.949 and 1 respectively.

Table3: Mean Sensitivity obtained through some segmentation approach

Segmentation Approach	Sensitivity
CNNs [29]	0.82
Urban et al. [32]	0.8
Havaei et al. [33]	0.8
CTSS [31]	0.84
OECM	0.98

Table 3 shows the mean value of Sensitivity that obtained through different segmentation approach on the BraTS datasets, where our OECM approach got 0.98 sensitivity, which is 14% more compare to CTSS [31] approach that, validate the performance of MRI image segmentation.

V. CONCLUSION

In this paper, we performed segmentation of brain tumor in MRI images, the used dataset is taken through BraTS 2013 segmentation challenge. An OECM approach is proposed that integrated with spatial regularization and LM for the tumor segmentation in MRI brain image, where the LM is consider to measure the distance for better representation of comparisons between surrounding voxels and the clustering distortion. Moreover, feature selection procedure is applied via a low dimensional transformation of feature and the larger segmented areas is consider for the tumor segmentation. The mean dice score obtained was 0.89 which conclude the proposed model efficiency. In the future work, the classification of segmented tumor can be performed to get the label of segmented tumor.

REFERENCES

1. S. Bauer et al., “A survey of MRI-based medical image analysis for brain tumor studies,” Phys. Med. Biol., vol. 58, no. 13, pp. 97–129, 2013.
2. E.G.Van Meiretal. , “Exciting new advances in neuro-oncology: The avenue to a cure for malignant glioma,”CA, Cancer J. Clinicians, vol. 60, no. 3, pp. 166–193, 2010.
3. B. Menze et al., “The multimodal brain tumor image segmentation benchmark (BRATS),” IEEE Trans. Med. Imag., vol. 34, no. 10, pp. 1993–2024, Oct. 2015.
4. N. J. Tustisonet al., “N4ITK: Improved n3 bias correction,” IEEE Trans .Med. Imag., vol.29, no.6 ,pp.1310–1320,Jun.2010.
5. L. G. Nyúl, J. K. Udupa, and X. Zhang, “New variants of a method of MRI scale standardization,” IEEE Trans. Med. Imag., vol. 19, no. 2, pp. 143–150, Feb. 2000.
6. M. Prastawa et al., “A brain tumor segmentation framework based on outlier detection,” Med. Image Anal., vol. 8, no. 3, pp. 275–283, 2004.
7. B. H. Menze et al., “A generative model for brain tumor segmentation in multi-modal images,” in Medical Image Computing and Comput. Assisted Intervention -MICCAI2010. NewYork: Springer, 2010, pp. 151–159.
8. D. Kwon et al., “Combining generative models for multifocal glioma segmentation and registration,” in Medical Image Computing and Comput.-Assisted Intervention-MICCAI 2014. New York: Springer, 2014, pp. 763–770.
9. S. Bauer, L.-P. Nolte, and M. Reyes, “Fully automatic segmentation of brain tumor images using support vector machine classification in combination with hierarchical conditional random field regularization,” in Medical Image Computing and Comput.-Assisted Intervention-MICCAI2011. New York: Springer, 2011,pp.354–361.
10. G. Thibault et al., “Advanced statistical matrices for texture characterization: application to cell classification,” IEEE Transactions on Biomedical engineering, vol. 61, no. 3, pp. 630–637, 2014.
11. J. Zhang et al., “Automatic craniomaxillofacial landmark digitization via segmentation-guided partially-joint regression forest model and multi-scale statistical features,” IEEE Transactions on Biomedical Engineering, vol. 63, no. 9, pp. 1820–1829, 2016.
12. F. Wang and J. Sun, “PSF: A unified patient similarity evaluation framework through metric learning with weak supervision,” IEEE Journal of Biomedical and Health Informatics, vol. 19, no. 3, pp. 1053–1060, 2015.
13. H. Jia et al., “A new distance metric for unsupervised learning of categorical data,” IEEE Transactions on Neural Networks and Learning Systems, vol. 27, no. 5, pp. 1065–1079, 2016.
14. G. Shafer, A mathematical theory of evidence. Princeton university press Princeton, 1976, vol. 1.
15. A. Roche et al., “On the convergence of EM-like algorithms for image segmentation using Markov random fields,” Medical Image Analysis, vol. 15, no. 6, pp. 830–839, 2011.
16. A. Criminisi and J. Shotton, Eds., Decision Forests for Computer Vision and Medical Image Analysis. Heidelberg, Germany: Springer, 2013.
17. C. Cortes and V. N. Vapnik, ‘‘Support vector networks,’’ Mach. Learn., vol. 20, no. 3, pp. 273–297, 1997.
18. F. Ye, J. Pu, J. Wang, Y. Li and H. Zha, "Glioma grading based on 3D multimodal convolutional neural network and privileged learning," 2017 IEEE International Conference on Bioinformatics and Biomedicine (BIBM), Kansas City, MO, 2017, pp. 759-763.
19. A. Gooya et al., ‘‘GLISTR: Glioma image segmentation and registration,’’ IEEE Trans. Med. Imag., vol. 31, no. 10, pp. 1941–1954, Oct. 2012.
20. W. E. Phillips, R. P. Velthuizen, S. Phuphanich, L. O. Hall, L. P. Clarke, and M. L. Silbiger, ‘‘Application of fuzzy c-means segmentation technique for tissue differentiation in MR images of a hemorrhagic glioblastoma multiforme,’’ Magn. Reson. Imag., vol. 13, no. 2, pp. 277–290, 1995.
21. R. Beare, ‘‘Regularized seeded region growing,’’ in Proc. 6th Int. Symp. Math. Morphol., 2002, pp. 91–99.
22. B. N. Li, C. K. Chui, S. Chang, and S. H. Ong, ‘‘Integrating spatial fuzzy clustering with level set methods for automated medical image segmentation,’’ Comput. Biol. Med., vol. 41, no. 1, pp. 1–10, 2011.
23. C. Li, R. Huang, Z. Ding, J. C. Gatenby, D. N. Metaxas, and J. C. Gore, ‘‘A level set method for image segmentation in the presence of intensity in homogeneities with application to MRI,’’ IEEE Trans. Image Process., vol. 20, no. 7, pp. 2007–2016, Jul. 2011.
24. A. Yezzi, S. Kichenassamy, A. Kumar, P. Olver, and A. Tannenbaum, ‘‘A geometric snake model for segmentation of medical imagery,’’ IEEE Trans. Med. Imag., vol. 16, no. 2, pp. 199–209, Apr. 1997.
25. R. A. Waltz et al., “An interior algorithm for nonlinear optimization that combines line search and trust region steps,” Mathematical Programming, vol. 107, no. 3, pp. 391–408, 2006.
26. A. Beck and M. Teboulle, “A fast iterative shrinkage-thresholding algorithm for linear inverse problems,” SIAM Journal on Imaging Sciences, vol. 2, no. 1, pp. 183–202, 2009.
27. http://martinos.org/qtim/miccai2013.
28. Huang M, Yang W, Wu Y, et al. Brain Tumor Segmentation Based on Local Independent Projection-Based Classification[J]. IEEE transactions on bio-medical engineering, 2014, 61(10):2633-45.
29. Pereira S, Pinto A, Alves V, et al. Brain Tumor Segmentation using Convolutional Neural Networks in MRI Images.[J]. IEEE Transactions on Medical Imaging, 2016, 35(5):1240-1251.

30. Cordier N, Menze B, Delingette H, et al. Patch-based Segmentation of Brain Tissues[C]// MICCAI Challenge on Multimodal Brain Tumor Segmentation, 2013, Nagoya, Japan, 2013.
31. Zhan, Tianming & Shen, Fangqing & Hong, Xunning & Wang, Xihu & Chen, Yunjie & Lu, Zhenyu & Yang, Guowei. (2018). A Glioma Segmentation Method Using CoTraining and Superpixel-based Spatial and Clinical Constraints. IEEE Access. PP. 1-1.
32. Urban G, Bendszus M, Hamprecht F A, et al. Multi-modal brain tumor segmentation using deep convolutional neural networks[C]// MICCAI BraTS (Brain Tumor Segmentation) Challenge. Proceedings, winning contribution. 2014.
33. Havaei M, Davy A, Warde-Farley D, et al. Brain tumor segmentation with Deep Neural Networks[J]. Medical Image Analysis, 2017, 35:18-31.

AUTHORS PROFILE:

Author-1

Nagaveni B Sangolgi
Dept.: ECE, Faculty of Engineering & Technology (Exclusively for Women), Sharnbasva University, Kalaburagi.
Designation: Asst. Prof
Email id: nagvenibs@rediffmail.com
Education M. Tech (Ph.D.)
Research work: Image processing
Publications: 2 international conferences.

Author-2

Name: **Dr. M. Sasikala**
Department: EEE
College name: Godutai Engineering College for women, Kalaburagi.
Designation: Principal

Email id: sasi_mun@rediffmail.com
Education: BE, ME, Ph.D.
Research work: Design of Fuzzy Logic controllers, design of sensors.
Honours and awards: Qualified GATE in 1985 for studyng ME
Gold medal for standing 1st in ME in. 1987
Publications: Technical 40
Papers accepted in national and international conference. 17